J. Biochem. 2011;149(4):463–474 doi:10.1093/jb/mvr006

JB THE JOURNAL OF BIOCHEMISTRY

Conformation of the calmodulin-binding domain of metabotropic glutamate receptor subtype 7 and its interaction with calmodulin

Received October 19, 2010; accepted December 21, 2010; published online January 21, 2011

Noriyoshi Isozumi[1,2], Yoshinori Iida[1,2], Akiko Nakatomi[3], Nobuaki Nemoto[4], Michio Yazawa[3] and S. Ohki[2,*]

[1]School of Materials Science; [2]Center for Nano Materials and Technology (CNMT), Japan Advanced Institute of Science and Technology (JAIST), 1-1 Asahidai, Nomi, Ishikawa 923-1292; [3]Graduate School of Science, Hokkaido University, N10 W8, Sapporo 060-1008; and [4]JEOL Co. Ltd., 3-1-2 Musashino, Akishima, Tokyo 196-8558, Japan

*S. Ohki, Center for Nano Materials and Technology (CNMT), Japan Advanced Institute of Science and Technology (JAIST), 1-1 Asahidai, Nomi, Ishikawa 923-1292, Japan. Tel: +81 761 51 1461, Fax: +81 761 51 1455, email: shinya-o@jaist.ac.jp

Calmodulin (CaM), a Ca^{2+}-binding protein, is a well-known regulator of various cellular functions. One of the targets of CaM is metabotropic glutamate receptor 7 (mGluR7), which serves as a low-pass filter for glutamate in the pre-synaptic terminal to regulate neurotransmission. Surface plasmon resonance (SPR), circular dichroism (CD) spectroscopy and nuclear magnetic spectroscopy (NMR) were performed to study the structure of the peptides corresponding to the CaM-binding domain of mGluR7 and their interaction with CaM. Unlike well-known CaM-binding peptides, mGluR7 has a random coil structure even in the presence of trifluoroethanol. Moreover, NMR data suggested that the complex between Ca^{2+}/CaM and the mGluR7 peptide has multiple conformations. The mGluR7 peptide has been found to interact with CaM even in the absence of Ca^{2+}, and the binding is directed toward the C-domain of apo-CaM rather than the N-domain. We propose a possible mechanism for the activation of mGluR7 by CaM. A pre-binding occurs between apo-CaM and mGluR7 in the resting state of cells. Then, the Ca^{2+}/CaM-mGluR7 complex is formed once Ca^{2+} influx occurs. The weak interaction at lower Ca^{2+} concentrations is likely to bind CaM to mGluR7 for the fast complex formation in response to the elevation of Ca^{2+} concentration.

Keywords: calmodulin/interaction/metabotropic glutamate receptor 7/multiple conformations/pre-binding.

Abbreviations: AMPA, α-amino-3-hydroxy-5-methyl-4-isoxazolepropinic acid; CaM, calmodulin; CaM-N (-C), N-terminal (C-terminal) half domain of CaM; CD, circular dichroism spectroscopy; EDTA, ethylenediaminetetraacetic acid; EGTA, ethylene glycol tetraacetic acid; IPTG, isopropyl-β-D-thiogalactopyranoside; MARCKS, myristoylated alanine-rich C kinase substrate; mGluRs, metabotropic glutamate receptors; NMDA, *N*-methyl-D-asparate; NMR, nuclear magnetic spectroscopy; PDE, phosphodiesterase; PKC, protein kinase C; smMLCK, smooth muscle myosin light chain kinase; SPR, surface plasmon resonance; TFE, trifluoroethanol.

Glutamate is one of the best-known excitatory neurotransmitters occurring in a wide variety of synapses in the central nervous system. Glutamate is recognized by two types of receptors (*1*): one is the so-called ionotropic glutamate receptors, including α-amino-3-hydroxy-5-methyl-4-isoxazolepropinic acid (AMPA), kainite and *N*-methyl-D-asparate (NMDA) types, which are responsible for fast neurotransmission. The other group, G-protein-coupled metabotropic glutamate receptors (mGluRs), influences various second messenger systems and ion channels in the regulation of synaptic transmission, neuronal development, and synaptic plasticity (*1–4*). mGluRs are anchored to the cell membrane and are composed of seven transmembrane domains (*5*). The N-terminal region of mGluRs contains a glutamate-binding domain and is exposed to the outside of the cell, while the C-terminal region is exposed to the cytosol. At least eight subtypes (mGluR1–8) have been identified and are classified into three groups (groups I–III) based on their sequence homology and properties related to second messenger coupling (*2*, *4*).

In this study, we focus on one mGluR subtype, mGluR7, which is mostly localized in pre-synaptic vesicle release sites in hippocampal neurons. mGluR7 is assumed to act as a low-pass filter at the axon terminal by inhibiting synaptic transmission upon high-frequency stimulation (*6*). Pharmacological and immunocytochemical studies had indicated that mGluR7 acts pre-synaptically to regulate neurotransmission in the hippocampus, and receptor knockout studies have suggested its role in regulating amygdala-dependent learning and memory (*7–9*). Besides the physiological characteristics of mGluR7, its functional mechanisms based on its structure have also been studied. The C-terminal region of group III mGluRs, except for mGluR6, has been reported to interact with calmodulin (CaM) in a calcium (Ca^{2+})-dependent manner (*10*). The Ca^{2+}/CaM-binding region of mGluR7 is conserved in group III mGluRs (*11–13*).

CaM, one of the key players in the signalling pathway via mGluR7, is a ubiquitous Ca^{2+}-binding protein that acts as a trigger of many enzymatic functions in cells. With increasing Ca^{2+} concentration in cells, one CaM molecule binds four Ca^{2+} ions. CaM has a dumbbell-like structure: it has two globular domains (N- and C-domains) connected by a flexible linker and both domains have 2 EF-hand-type Ca^{2+} binding sites. The C-domain has higher affinity for Ca^{2+} compared to the N-domain. Binding of Ca^{2+} to CaM exposes its hydrophobic residues to the molecular surface, and these hydrophobic residues are responsible for binding to the target molecule (*14*, *15*).

Target recognition of Ca^{2+}/CaM has been extensively studied, and numerous CaM-targeting enzymes have been discovered (*14*, *15*). The CaM-binding motifs of CaM-targeting enzymes are normally composed of 20–30 amphiphilic amino acid residues, classified into several groups, such as 1–10, 1–14, 1–16 etc. (*16*, *17*). This classification is based on the position of key residues in the CaM-binding motifs for interaction with Ca^{2+}/CaM. For example, smooth muscle myosin light chain kinase (smMLCK) is one of the CaM-targeting enzymes whose CaM-binding region is composed of 20-amino acid residues (ARRKWQ KTGHAVRAIGRLSS). In this case, Trp, Val and Leu are anchored to Ca^{2+}/CaM. The binding manner is classified as the 1-8-14 type, where Val and Leu are the 8th and 14th residues, respectively, while Trp is the first. The smMLCK peptide assumes an α-helix formation when in complex with Ca^{2+}/CaM (*18*).

The mGluR7 region from residue 856 to 879 was recently identified to be responsible for CaM binding (*19*). Previous biochemical studies suggested that binding of the mGluR7 peptide (856–879) to CaM occurs in a Ca^{2+}-dependent manner and has a 1 : 1 stoichiometry (*13*, *19*). Residual dipolar coupling constants were estimated from nuclear magnetic spectroscopy (NMR) experiments on the Ca^{2+}/CaM-mGluR7 complex. The NMR data suggest that the overall molecular shape of the Ca^{2+}/CaM-mGluR7 complex is very close to that of Ca^{2+}/CaM-smMLCK. Therefore, it was proposed that the mGluR7 peptide binds to Ca^{2+}/CaM in a 1-8-14 manner (*19*, *20*).

Notably, in the primary structure of mGluR7, a part of the CaM-binding region is reserved for binding to the G-protein βγ subunit (*13*). Furthermore, it had reported that the Ca^{2+}/CaM binding to type III mGluRs inhibits its phosphorylation caused by protein kinase C (PKC) on a serine residue involved in the Ca^{2+}/CaM-binding region (*21*). Thus, the CaM-binding region of mGluR7 is recognized by at least three different functional proteins (*i.e.* CaM, G-protein βγ–subunit and PKC). The physiological role of such competition among PKC, Ca^{2+}/CaM and G-protein βγ–subunit remains unclear. In this article, to characterize the biochemical and biophysical properties of this multifunctional segment in mGluR7, we performed detailed analyses by using surface plasmon resonance (SPR), circular dichroism (CD) spectroscopy, and NMR. In addition, the interaction of the mGluR7 peptide with CaM is also discussed with the aim to fully understand its biological function.

Materials and Methods

Samples

Peptides corresponding to the CaM-binding region of mGluR7, short (residues 856–875; VQKRKRSFKAVVTAATMSSR) and long (residues 856–879; VQKRKRSFKAVVTAATMSSRLSHK) peptides, were expressed and purified according to previously described methods (*22*). For the SPR experiments, tag cleavage was not performed.

Unlabelled and uniformly labelled samples of intact and each half of CaM (CaM-N, residues 1–77; and CaM-C, residues 78–148) were prepared according to previously published methods (*23*, *24*). The CaM sample with [^{13}C methyl]-Met–selective labelling was prepared as follows. *Escherichia coli* was used for CaM expression. The bacteria were cultured in M9 medium until $A_{600} = 0.3$; then, an amino acid mixture composed of Tyr, Phe, Leu, Ile, Val and [^{13}C-methyl]-Met (100 mg each for 1 l culture medium) was added into the culture. Protein production was induced by the addition of isopropyl-β-D-thiogalactopyranoside (IPTG) into the medium at $A_{600} = 0.6$. After 4 h of shaking at 37°C, the culture medium was harvested. Purification of the [^{13}C-methyl]-Met–labelled CaM was carried out in accordance with the method used for other CaM samples.

SPR analyses

The interaction of CaM with mGluR7 was monitored using Biacore J (GE Healthcare). Sensor Chip CM5 was used to immobilize the tag-mGluR7 peptide by amine coupling. CaM samples in at least five different concentrations (0.5–200 μM and 0.01–10 mM CaM in the presence and absence of Ca^{2+}, respectively) were examined in each experiment. The experimental condition was as follows: running buffer A [20 mM BisTris–HCl, 300 mM KCl and 1 mM $CaCl_2$ (pH 6.8)] or B [20 mM BisTris–HCl, 300 mM KCl, 1 mM $MgCl_2$ and 3 mM EGTA (pH 6.8)] was eluted at a flow rate of 30 μL/min with a CaM injection time of 120 s. The experiments were carried out at 25°C. The dissociation constants were calculated with BIA evaluation in the kinetic analysis mode; simultaneous fitting by 1 : 1 binding with a mass transfer model was performed. When kinetic analysis failed, the K_D values were calculated using the affinity analysis mode.

CD measurements

CD spectra were recorded at from 260 to 200 nm using a JASCO J-820 spectrophotometer with a temperature-jacketed spectral cell of 1 mm cell path length. CD measurements were performed at 25°C for 10 μM CaM and/or 10 μM mGluR7 peptide dissolved in 10 mM Tris–HCl, 100 mM KCl and 0.1 mM $CaCl_2$ (pH 6.8). The samples containing trifluoroethanol (TFE) were prepared at a concentration of 10 μM mGluR7 peptide and measured at 25°C.

NMR experiments

The NMR sample buffer, except for [^{13}C-methyl]-Met–labelled CaM, was composed of 20 mM BisTris–HCl, 300 mM KCl, 10 mM $CaCl_2$ or 10 mM EDTA, 0.05% NaN_3 and 10% D_2O (pH 6.8). For [^{13}C-methyl]-Met–labelled CaM, the sample was dissolved into the buffer containing 20 mM Tris–HCl, 100 mM KCl, 10 mM $CaCl_2$ or 10 mM EDTA, 0.05% NaN_3 and 5% D_2O (pH 7.0). The protein concentration was approximately 0.5–1.0 mM, calculated using the value of A_{280}. The temperature of the sample was kept at 32°C and/or 25°C during the NMR experiments.

All NMR data for the resonance assignment of CaM in the complex were obtained on a JEOL ECA 600 spectrometer. Other NMR experiments were performed on a Varian INOVA 750 spectrometer with a Z-axis gradient triple-resonance probe and/or on a Bruker AVANCE III 800 spectrometer with a TCI cryogenic probe. The FID data were processed with NMRPipe (*25*) and analysed with Sparky (*26*).

Results

The C-domain of CaM is the dominant binding site of mGluR7

Previous reports that used spectrofluorometry and gel filtration suggested that mGluR7 (851–915), (851–888)

and (851–875) interact with Ca^{2+}/CaM in a 1 : 1 stoichiometric manner (*13*, *19*). We used SPR analyses to obtain further biophysical information on the interaction. For the SPR experiments, we used two kinds of mGluR7 peptides (*i.e.* with different lengths). Based on the assumption that the binding fits the 1-8-14 type, the longer peptide (residues 856–879) contains all hydrophobic residues necessary for binding, while the shorter peptide (residues 856–875) lacks a Leu residue at the 14th position. We expected that the experiments would show the effect of the last residue on the binding, and that the results could provide hints about the structure of the complex.

Figure 1 and Table I show the results of the SPR experiments and the K_D values estimated from the SPR data. Figure 1A and D clearly shows that both mGluR7 peptides were able to bind to intact CaM in the presence of Ca^{2+}, and the longer one exhibited higher affinity than that of the shorter one. The dissociation constant (K_D) was estimated as $(7.29 \pm 1.82) \times 10^{-9}$ and $(2.55 \pm 0.68) \times 10^{-8}$ M for the long and short peptides, respectively (Table I). These values are consistent with previously reported K_D values estimated by spectrofluorometry and isothermal titration calorimetry (*10*, *13*, *19*). The longer peptide has about five times smaller K_D value for the Ca^{2+}-bound CaM compared to the shorter peptide. Thus, deletion of four residues at the C-terminal region of the mGluR7 peptide decreases its binding affinity, suggesting that this region contains the key residue(s) for binding.

Interestingly, this decreased affinity depending on the peptide length is also observed for the two half-CaM fragments corresponding to the N- and C-domains. The K_D of the N- and C-domain fragments is about three and two times greater, respectively, when the shorter peptide was used. Based on these results, it is suggested that both CaM fragments possibly interact with the C-terminal region of the mGluR7 peptide. Figure 1B, C, E and F shows the results of half-CaM fragments. The comparison of B with C and E with F suggests that the C-domain of CaM binds more strongly to the mGluR7 peptide than the N-domain. This pattern is observed for both mGluR7 peptides.

The interaction between CaM and its targets was also examined in the absence of Ca^{2+}. The K_D values in all experiments are summarized in Table I. Weak binding was observed in all cases in the absence of Ca^{2+}. Especially for the N-domain, accurate K_D values were not estimated because of the very weak binding; however, the interactions were detected in both peptides (Fig. 1G). Most noticeably, the difference in the binding properties of the two domains becomes greater compared to those monitored in the presence of Ca^{2+}. The N-domain shows quite a low affinity for both peptides, but the C-domain has affinity for both peptides with K_D in the submicromolar range. The data suggests that the C-domain of CaM interacts with mGluR7 even in the absence of Ca^{2+}. In the SPR studies, mGluR7 peptides, of which N-terminal ends are conjugated to an affinity tag, were used. The ^{1}H-^{15}N HSQC spectrum of ^{15}N-labelled CaM with mGluR7 (856–879) peptide (Fig. 5B) was the same as the spectrum of ^{15}N-labelled CaM with the tag-peptide (data not shown). Therefore, it seems that the CaM–mGluR7 interaction is not influenced by the tag peptides.

The mGluR7 peptide is in random conformation

Because the binding of mGluR7 to Ca^{2+}/CaM had been predicted to be of the 1-8-14 type, which is similar to smMLCK, a previous conformational study on the smMLCK peptide may provide hints about the conformational preference of the mGluR7 peptide (*18*). To compare with the previous results on the smMLCK peptide, we performed CD experiments for mGluR7 (856–879). TFE/aqueous solutions are known to stabilize the secondary structure of peptides, especially for α-helices (*27*, *28*). Therefore, we measured the CD spectra in the absence and presence of TFE. Figure 2A shows the CD spectra of the peptide dissolved in various concentrations of TFE/aqueous solutions. In the absence of TFE, mGluR7 (856–879) is suggested to be in random conformation. This is the popular conformation of CaM-binding peptides in aqueous solution. The CD spectra of mGluR7 (856–879) changed with increasing concentrations of TFE. The decrease in ellipticity at 222 nm, which is the index of α-helices, suggests that some helical conformation is stabilized with increasing TFE concentration. However, the helix content is estimated to be 24% in 50% TFE/aqueous solution. This poor ability to form helices is very different from the properties of well-known CaM-binding peptides. Only few reports on other CaM-binding peptides provide similar random conformation (*29–31*).

Furthermore, we observed the CD spectra of the complex between Ca^{2+}/CaM and the mGluR7 peptide (Fig. 2B). Because apo-CaM dose not change its secondary structure remarkably when it interacts with peptides, the difference spectrum can be attributed to the peptide bound to apo-CaM (*32*, *33*). As shown in Fig. 2B, the addition of mGluR7 peptide hardly influences the ellipticity at 222 nm, the index of α-helices. It is confirmed that the poor absorption at 222 nm is observed in the difference spectrum. Thus, it is suggested that, even in the complex with Ca^{2+}-saturated CaM, the mGluR7 peptide does not form a stable α-helical conformation, but forms a partial α-helix and/or the whole molecular structure is in equilibrium between random and helical conformations.

The CD results prompted us to perform NMR analysis of the mGluR7 peptides to confirm the conformation of mGluR7 bound to CaM. We prepared ^{15}N-labelled peptides and obtained the NMR spectra. Figure 3A shows the NMR spectra of mGluR7 (856–879) alone. In the aqueous solution, the mGluR7 peptide gives signals within a narrow range in both dimensions of ^{1}H-^{15}N HMQC. Next, the effect of TFE on the peptide conformation was examined by NMR. The NMR spectrum of mGluR7 (856–879) in 50% TFE (Fig. 3B) was different from that in the absence of TFE (Fig. 3A). The NMR result suggests that the structural change of mGluR7 peptide was induced by TFE. This result supports the CD result described

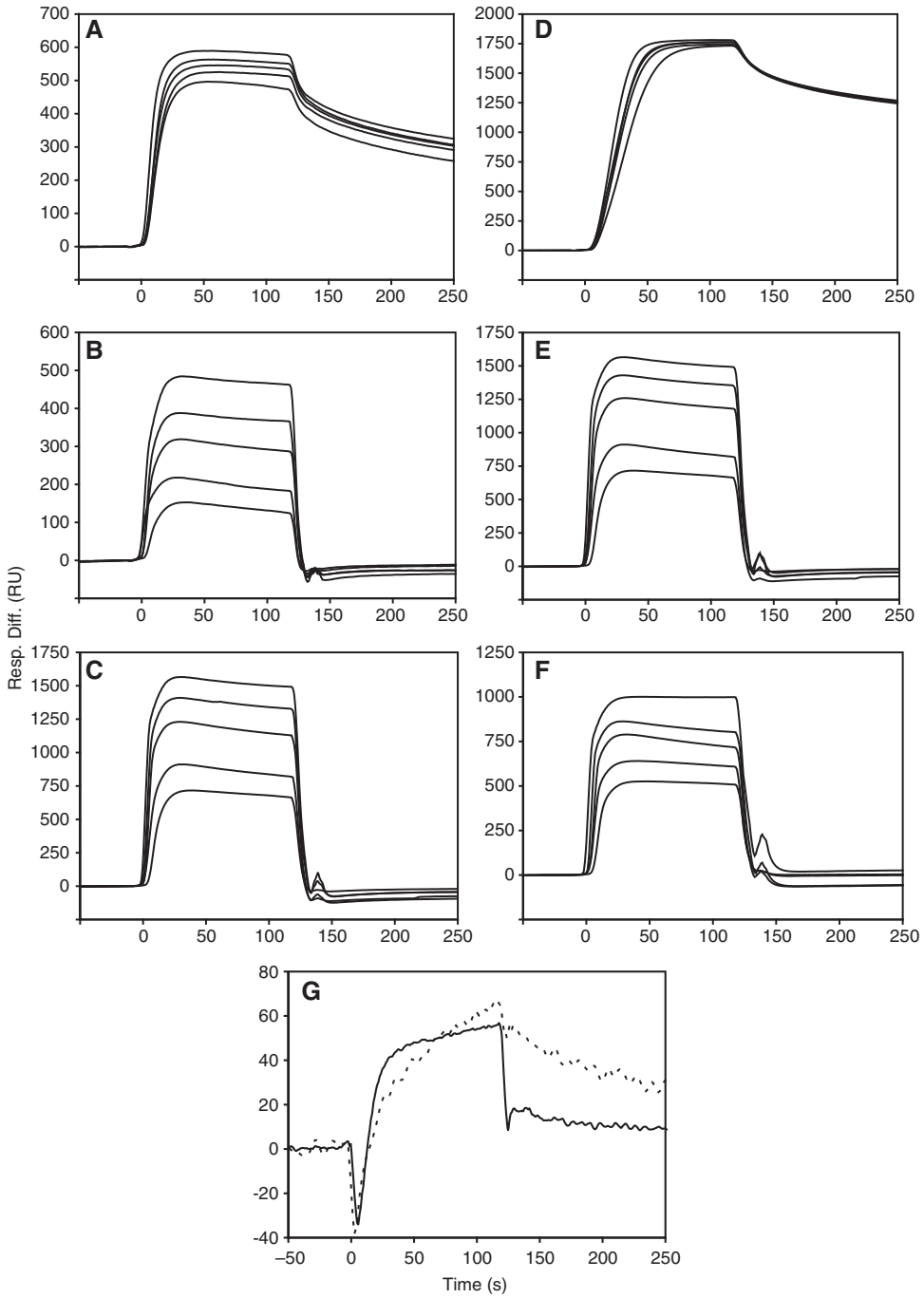

Fig. 1 SPR spectra of mGluR7 with Ca^{2+}/CaM. mGluR7 (856–879) was immobilized and injected with full-length CaM (A), CaM-N (B), and CaM-C (C). mGluR7 (856–875) was immobilized and injected with full-length CaM (D), CaM-N (E), and CaM-C (F). In each experiment, the results from experiments using five concentrations of CaM are superimposed on a spectrum. (G) In the absence of Ca^{2+}, 200 μM CaM-N was injected to immobilized mGluR7 (856–879) (solid line) and mGluR7 (856–875) (dashed line).

above. However, the spectrum of mGluR7 in 50% TFE provided too many peaks compared to the number of its amino acid residues. This strongly suggests that the mGluR7 peptide has multiple conformations even in 50% TFE.

NMR experiments of ^{15}N-labelled mGluR7 (856–879) peptide in the absence and presence of unlabelled apo-CaM were preformed. Comparison of the two spectra (Fig. 4A and B) showed that the peaks of the peptide in ^{1}H-^{15}N HSQC were slightly changed by addition of apo-CaM. Although the 3D NMR measurement was carried out, it was difficult to assign the weak signals. Therefore, the interaction is further examined using labelled CaM as describe latter.

Another NMR experiment, titration of ^{15}N-labelled mGluR7 peptide with Ca^{2+}/CaM, was also carried out. The result is shown in Fig. 4C. Resonance assignment was carried out using ^{15}N-edited NOESY and TOCSY. Only the region from R861 to K879 was

assigned because the intensities of some peaks were too weak. Continuous $d_{\alpha N}(i, i+3)$ NOEs indicating formation of an α-helix were undetected in ^{15}N-edited NOESY, and CSI values for ^{1}Hα were in the random-coil range (Supplementary Fig. S1; *34*). Such NMR parameters suggest the random conformation of the peptide in aqueous solution. Because the SPR experiments suggested tight binding between the mGluR7 peptide and Ca^{2+}/CaM, we expected simple spectral transition such as slow exchange. However, the NMR data were complex and unclear. This spectrum is different from those of the peptide alone and the peptide in the presence of apo-CaM, suggesting that the binding to Ca^{2+}/CaM induces some conformational change of mGluR7 peptide.

Table I. Dissociation constant (K_D) of CaM and mGluR7 peptides.

	K_D (M)	
Sample	**mGluR7 (856–879)**	**mGluR7 (856–875)**
In the presence of Ca^{2+}		
CaM-FL	$(7.29 \pm 1.82) \times 10^{-9}$[a]	$(2.25 \pm 0.68) \times 10^{-8}$[a]
CaM-N	$(8.11 \pm 0.05) \times 10^{-6}$	$(2.03 \pm 0.09) \times 10^{-5}$
CaM-C	$(4.59 \pm 0.83) \times 10^{-6}$	$(9.18 \pm 1.12) \times 10^{-6}$
In the absence of Ca^{2+}		
CaM-FL	$(2.19 \pm 0.90) \times 10^{-4}$	$(1.06 \pm 0.23) \times 10^{-3}$
CaM-N	ND	ND
CaM-C	$(2.54 \pm 1.21) \times 10^{-4}$	$(3.84 \pm 0.86) \times 10^{-4}$

The sample condition was as follows: (i) 20 mM BisTris–HCl, 300 mM KCl, 1 mM $CaCl_2$ (pH 6.8); (ii) 20 mM BisTris–HCl, 300 mM KCl, 1 mM $MgCl_2$, 3 mM EGTA (pH 6.8). ND means 'not determined,' because the estimated value is too large to evaluate correctly.

[a]The K_D values were estimated through the kinetic analysis mode. When the relative weak interaction provides a K_D value that is higher than 10^{-6} M, K_D values were estimated through the affinity analysis mode. (The affinity analysis mode is more suitable than the kinetic analysis mode for evaluation of weak interactions.).

CaM bound to mGluR7 peptide has multiple conformations

To obtain further experimental results to support the data described above, we used ^{15}N-labelled CaM for alternative NMR experiments. Figure 5A shows the ^{1}H-^{15}N HSQC spectrum of ^{15}N-labelled apo-CaM bound to the unlabelled mGluR7 peptide. The boxes in the spectrum indicate positions of the peaks that disappeared. The spectrum shows that local conformation around F89, N97, S101 and E139 was changed upon the interaction with the mGluR7 peptide. At the lower concentration of mGluR7 peptide, peaks for the C-domain, rather than the N-domain, were changed. The spectral change is detected at [peptide]/[CaM] = 1 (Fig. 5B). Moreover, in the spectrum at

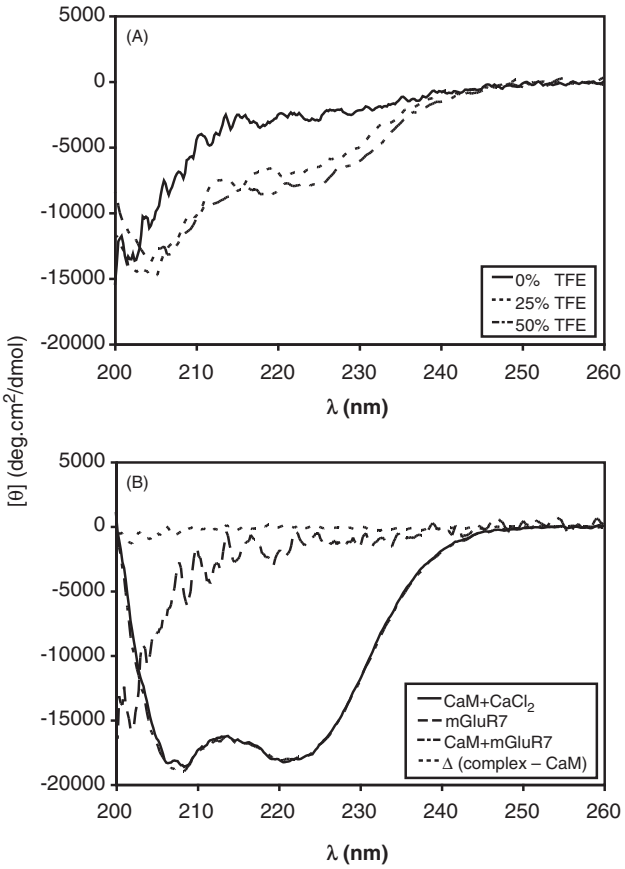

Fig. 2 Far-UV CD spectra of mGluR7 peptide, Ca^{2+}/CaM and the Ca^{2+}/CaM-mGluR7 peptide complex. (A) Spectra of mGluR7 (856–879) in 0% TFE (solid line), 25% TFE (dotted line), and 50% TFE (dashed/dotted line). (B) Spectra of Ca^{2+}/CaM (solid line), mGluR7 (856–879) (dashed line), Ca^{2+}/CaM-mGluR7 (856–879) complex (dashed/dotted line), and the difference spectrum between the Ca^{2+}/CaM-mGluR7 complex and Ca^{2+}/CaM (dotted line). The CD intensities are expressed as the mean residue molar ellipticity.

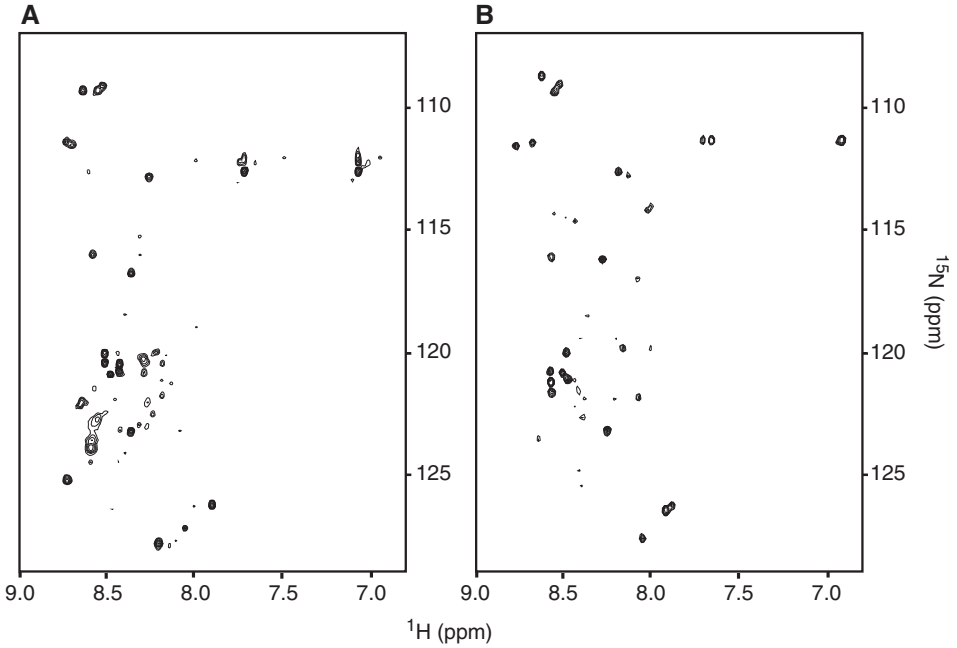

Fig. 3 ^{1}H-^{15}N HMQC spectra of ^{15}N-labelled mGluR7 (856–879). (A) Spectrum of mGluR7 peptide in 0% TFE. (B) Spectrum of mGluR7 peptide in 50% TFE. Temperature and pH of both samples were 32°C and pH 6.8, respectively.

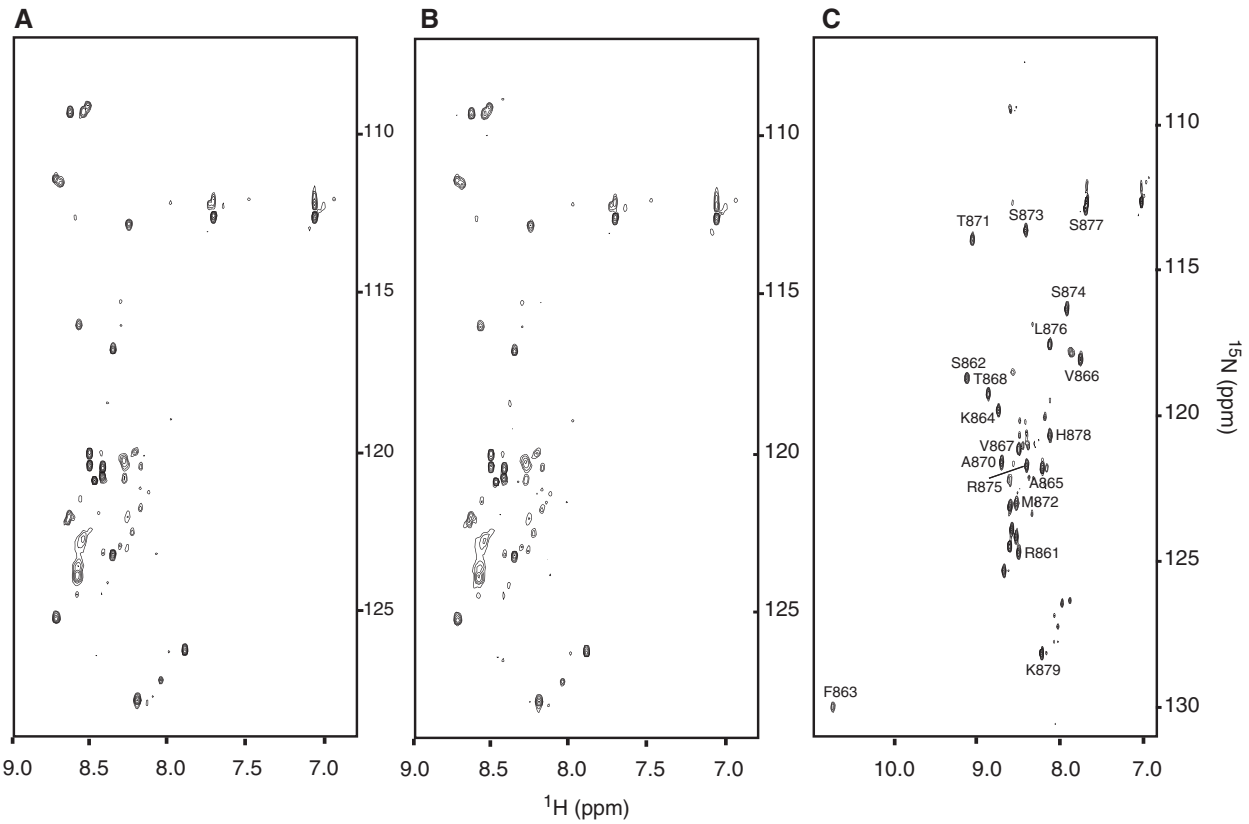

Fig. 4 ^{1}H-^{15}N HSQC spectra of ^{15}N-labelled mGluR7 (856–879) with CaM. (A) Spectrum of mGluR7 peptide alone. (B) Spectrum of mGluR7 peptide with apo-CaM at a 1 : 1 ratio. (C) Spectrum of mGluR7 peptide with Ca^{2+}/CaM at a 1 : 1 ratio. Partial assignments are labelled with the respective amino acid residues and numbers in (C). All samples were adjusted at pH 6.8, and the sample temperature were kept at 32°C during the experiments.

[peptide]/[CaM] = 3, some of the peaks, such as M109, D131, N137 and M145, disappeared (Fig. 5B). These residues are located in the C-domain of CaM. Furthermore, some peaks corresponding to the N-domain of CaM became weak at higher peptide concentrations. Thus, it is suggested that the C-domain of apo-CaM mainly interacts with the mGluR7 peptide. We also performed ^{1}H-^{15}N HSQC titration

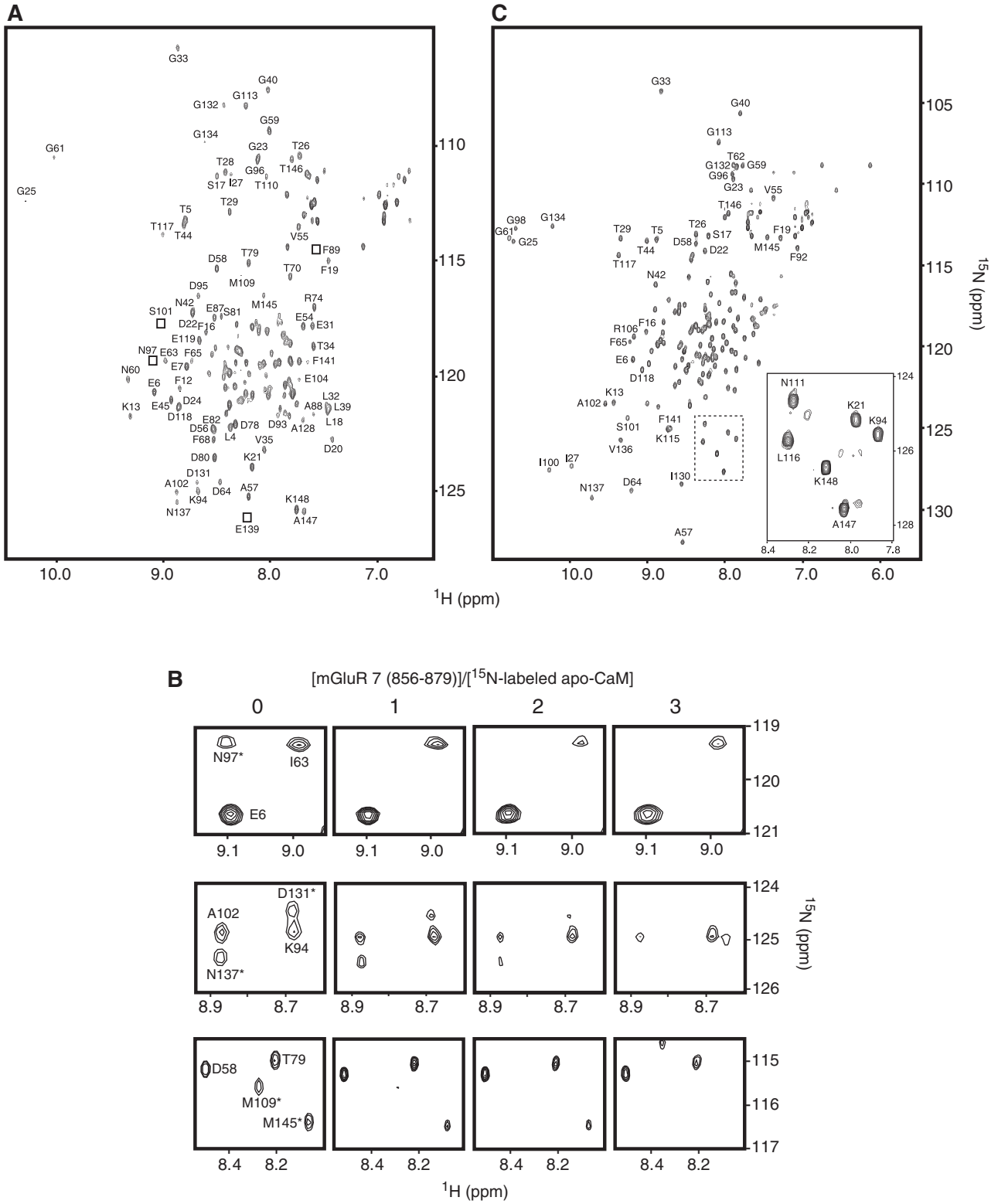

Fig. 5 ^{1}H-^{15}N HSQC spectra of ^{15}N-labelled CaM with mGluR7 (856–879). (A) Spectrum of apo-CaM with the peptide at a 1 : 1 ratio. Boxes present the resonance that disappeared upon the addition of the mGluR7 peptide. (B) Titration of apo-CaM with mGluR7 (856–879). ^{1}H-^{15}N HSQC spectra of [peptide]/[^{15}N-labelled apo-CaM] = 0–3 are displayed. Asterisks present the resonance that disappeared upon the addition of the mGluR7 peptide. (C) Spectrum of Ca^{2+}/CaM with the peptide at a 1 : 1 ratio. The expanded view, shown in the figure, corresponding to the dashed-line box is depicted at lower threshold. Assignments reported previously are labelled with the respective amino acid residues and numbers in all panels. Temperature of all samples adjusted at pH 6.8 was kept at 32°C through the experiments.

experiments of ^{15}N-labelled Ca^{2+}-bound CaM with the unlabelled mGluR7 peptide (Fig. 5C). This spectrum is totally different from the spectrum of Ca^{2+}/CaM alone, suggesting that the both domains of Ca^{2+}/CaM are involved in the binding to mGluR7. The NMR spectrum at higher threshold is identical to the result of previous report (*19*). However, the spectrum has a lot of minor peaks at lower threshold as shown in the expanded view in Fig. 5C. This suggests a possibility that the Ca^{2+}/CaM in the complex have minor conformations. Because of the weak intensities, it was hard to assign these minor signals, thus far the detail is unclear.

To obtain further structural information, we performed ^{1}H-^{13}C HSQC experiments monitoring side chains of nine Met residues. CaM has nine Met residues at 36, 51, 71, 72, 76, 109, 124, 144 and 145. The relatively long unbranched hydrophobic side chains of Met residues in CaM are responsible for the target binding (*35*, *36*). The methyl group of these Met residues has been reported to be a useful NMR probe for monitoring of target binding (*36*, *37*). Hence, we prepared [^{13}C-methyl Met]-CaM for the present work. The expression of [^{13}C-methyl Met]-CaM is straightforward, as described in the 'Materials and Methods' section. The purification protocol of [^{13}C-methyl Met]-CaM was exactly identical to that of unlabelled and/or uniformly labelled CaM. Mass spectrometry suggested that all Met residues were labelled with ^{13}C-methyl-Met (data not shown). Figure 6 displays the results of titration of [^{13}C-methyl Met]-CaM with the mGluR7 peptide. The methyl region of ^{1}H-^{13}C HSQC of [^{13}C-methyl Met]-CaM in the absence and presence of Ca^{2+} is shown in Fig. 6A and C. Both conditions clearly show nine Met signals, and the spectra were identical to those reported previously. Both NMR spectra were changed with the addition of the mGluR7 (856–879) peptide (Fig. 6B and D). As shown in Fig. 6B, the data for apo-CaM show that residues 109, 124 and 144 were intensely affected by the addition of the mGluR7 peptide. The results clearly indicate that the interaction mainly occurs in the C-domain of apo-CaM. The spectral change occurs in a fast- or intermediate-exchange manner, suggesting that the binding is relatively weak. In contrast to apo-CaM, the spectral change for Ca^{2+}/CaM is complicated. Strong peaks appeared at slightly shifted chemical shift positions compared to those for Ca^{2+}/CaM alone. Especially, the differences of the C-domain of Ca^{2+}/CaM seem greater than those of the N-domain. This result suggests that the C-domain of Ca^{2+}/CaM binds more strongly to the mGluR7 peptide in the complex, and is consistent with our SPR result and previous report (*19*). However, new small peaks appeared in the spectra. At the [peptide]/[CaM] ratio of 1:1, it is expected that all CaM are in the complex because the K_D is in the nanomolar range. The fact that more than nine peaks were detected in the NMR spectrum at the [peptide]/[CaM] ratio of 1:1 also suggests that Ca^{2+}/CaM interacting with mGluR7 peptide is in equilibrium among multiple conformations.

Discussion

Apo-CaM binding with mGluR7

Some CaM targets have been reported to interact with apo-CaM, including neurogranin, neuromodulin, PEP-19 and others (*38–40*). Some of these targets, such as α-syntrophin, inducible nitric oxide synthase (iNOS) and glycogen phosphorylase b kinase (Gbk), interact with CaM both in the absence and presence of Ca^{2+} (*41–43*). Although the number of studies on apo-CaM binding targets is currently increasing, the binding mode of apo-CaM to its targets is poorly characterized. In the present study, except for the NMR study on the ^{15}N-labelled peptide side, all results indicate that apo-CaM can interact with mGluR7. Interestingly, the C-domain of apo-CaM, which has a higher Ca^{2+} affinity, is the major site for this interaction. The weak interaction could keep CaM close to the mGluR7 peptide. Such inhomogeneous distribution of CaM in cells would contribute to the fast activation of mGluR7 after the elevation of Ca^{2+} concentration. Furthermore, the weak interaction can possibly prevent the binding of the G-protein βγ-subunit and PKC to mGluR7.

Comparison with other apo-CaM binding models

The hydrophobic residues responsible for the target binding are buried from the solvent-accessible molecular surface of apo-CaM. Thus, it seems that target sequences binding to apo-CaM would have different characteristics from those that bind to Ca^{2+}/CaM (*44*). Titration of ^{15}N-labelled apo-CaM with the mGluR7 peptide revealed that the affected peaks correspond to hydrophobic and hydrophilic residues. Thus, there is a possibility that the binding between apo-CaM and mGluR7 involved hydrophobic and/or electrostatic interactions.

Phosphodiesterase (PDE) is known as one of the targets that can bind to both apo-CaM and Ca^{2+}-bound CaM. The peptides comprising the CaM-binding region of PDE were demonstrated to bind solely to the C-domain of apo-CaM. Thus, it is likely that only electrostatic interactions exist between apo-CaM and PDE in the complex because the hydrophobic residues forming the binding surface on Ca^{2+}/CaM are buried within the interior of the domain in the α-helical conformation of apo-CaM (*45*). However, the mode of binding between apo-CaM and the PDE peptide is unknown until now. In the absence of Ca^{2+}, residues in the C-domain of apo-CaM binding to the PDE peptide gave broad peaks in ^{1}H-^{13}C HMQC. This is similar to our observations in ^{1}H-^{13}C HSQC for apo-CaM titrated with the mGluR7 peptide. Therefore, the modes of apo-CaM binding of PDE and mGluR7 may be categorized into a similar type.

Among the apo-CaM-binding peptides is a group referred to as the IQ motif (IQXXXRGXXXR, where X is any type of amino acid residue). The IQ motif is rather loosely adhered to in many cases. For example, Ile located at the first position is frequently replaced by Leu or Val or Met. The Arg residues at both the sixth position and the

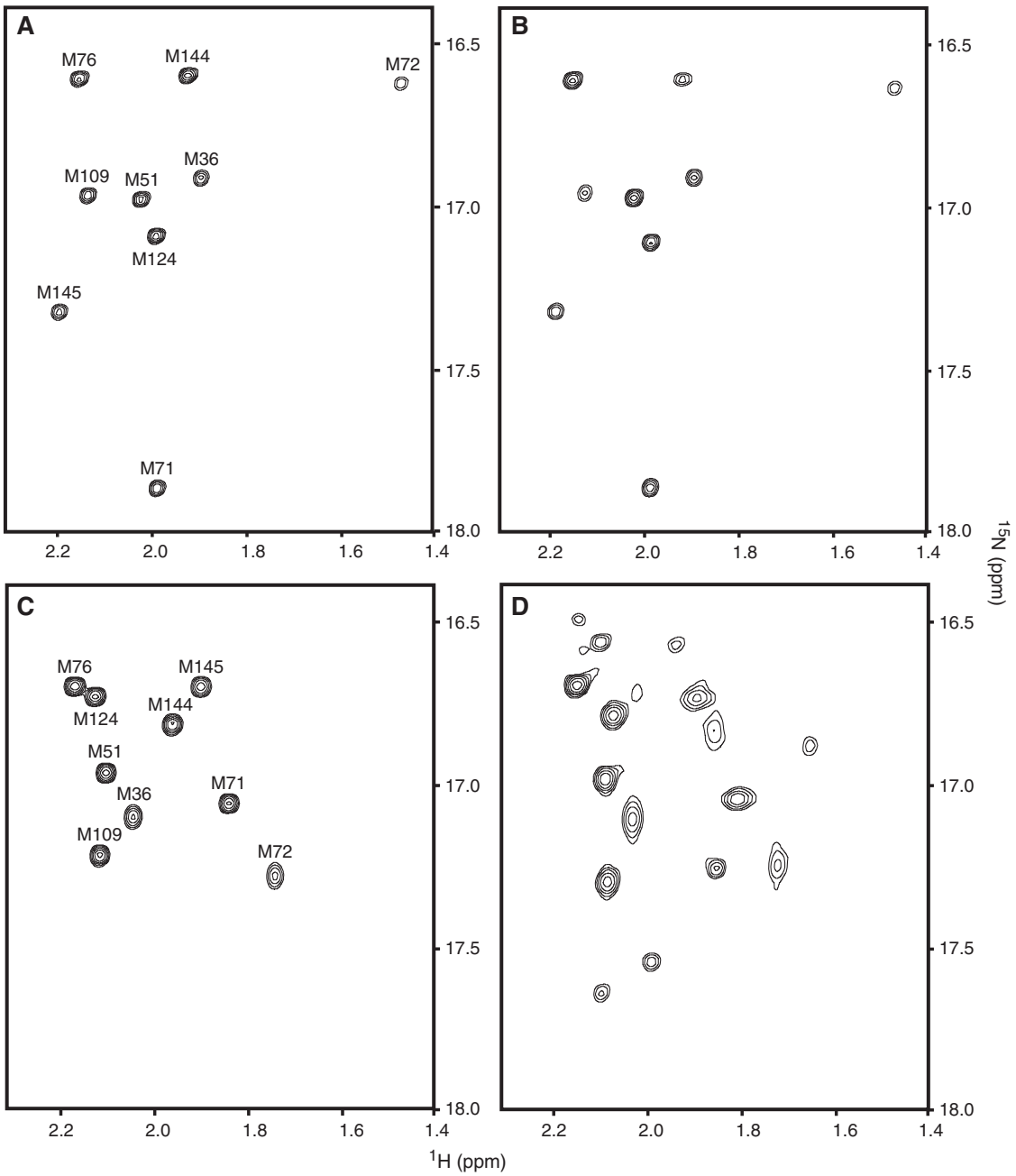

Fig. 6 ^{1}H-^{13}C HSQC spectra of ^{13}C-methyl Met-CaM. Spectra of apo-CaM (A) and with mGluR7 (856–879) (B). Spectra of Ca^{2+}/CaM (C) and with mGluR7 (856–879) (D). In (A and C), the assignments reported previously are labelled with the respective amino acid residues and numbers (*36*, *37*). In (B), the ratio of apo-CaM to peptide is 1 : 1.1 (black). In (D), the ratio of Ca^{2+}/CaM to peptide is 1 : 1.1. During the measurements, temperature of samples adjusted at pH 7.0 was kept at 25°C.

C-terminal-end positions are sometimes replaced by Lys or His. Gly often appears at the seventh position, but is not well conserved. When the target containing the IQ motif binds to apo-CaM, the target peptide forms an α-helical structure. It is known that the C-terminal half of IQ motif (IQXXXR) interacts with the C-domain of CaM and the N-terminal half of IQ motif (GXXXR) binds to the N-domain of CaM (*46*). Moreover, it is predicted that the incomplete IQ motif containing only first part (IQXXXR) also binds to apo-CaM (*47*). As compared with the IQ motif, the mGluR7 peptide has the sequence (VQKRKR, 856–861), similar to the C-terminal of the IQ motif. Thus, the VQKRKR sequence, containing basic residues, possibly interacts with apo-CaM.

CaM is known as an acidic protein, and the mGluR7 peptide used in this study had a number of basic residues. Thus, electrostatic interaction would be expected as a major binding force between apo-CaM and the mGluR7 peptide. A simple electrostatic interaction, as seen in the binding of the CH domain of SMTNL1 (*48*), could exist for the interaction of the mGluR7 peptide.

Role of each domain of Ca^{2+}/CaM in mGluR7 binding

The SPR results show that Ca^{2+}/CaM interacts with the mGluR7 peptides and the K_D is estimated in the subnanomolar range. The binding of the C-domain of Ca^{2+}/CaM to the mGluR7 peptide is dominant for the interaction. Such differential binding modes of the two domains may be related to the target activation mechanism of CaM. In the classic CaM-peptide binding model, contacts between the anchor residues of the peptide and the Met-rich hydrophobic binding pockets of Ca^{2+}/CaM are essential for high-affinity interactions. Many CaM-binding domains have a bulky hydrophobic residue at the first conserved position in the binding motif that has a higher affinity for the C-domain of CaM (*44*, *49*). This interaction with the C-domain of CaM is believed to be the initial binding step for target activation (*44*). The mGluR7 peptide has a Phe residue at position F863. It was reported that the substitution mutant of mGluR7 (F863A) does not bind to Ca^{2+}/CaM, and the phosphorylation of S862, neighboring F863, markedly weakens the binding to Ca^{2+}/CaM (*11*, *13*, *19*). Thus, the initial step of the interaction between mGluR7 and Ca^{2+}/CaM may be introduced by the binding of a bulky hydrophobic residue F863 of mGluR7 to the hydrophobic pocket of the C-domain of Ca^{2+}/CaM.

Binding mode of Ca^{2+}/CaM with mGluR7

The mGluR7 peptide does not form a complete helical conformation in the Ca^{2+}/CaM-mGluR7 complex. Furthermore, the complex between the mGluR7 peptide and Ca^{2+}/CaM does not have a stable single conformation. Thus, the binding type is different from the 1-8-14 motif (*16*, *18*, *50*). The 1-8-14 class is a classic model for the stable complex conformation in which the anchor residues of the helical peptide are located within the hydrophobic pockets of Ca^{2+}/CaM. If we adapt 1-8-14 binding to the mGluR7 peptide, the eighth position is Ala. The short side chain could contribute to the unique binding mode of mGluR7. The multiplicity of the complex structure may be the key for its function.

Possible activation mechanism

In this article, we investigated the interaction between CaM and mGluR7 in the absence and presence of Ca^{2+}. Based on the present results, we propose a possible activation mechanism: mGluR7 interacts with the C-domain of apo-CaM at very low Ca^{2+} concentrations in cells. Such pre-binding would be effective in pre-synaptic terminals to achieve rapid regulation of neurotransmitter release and synaptic vesicle recycling against the Ca^{2+} influx occurring in the millisecond range (*51*). Further analyses at cell level are necessary to confirm this pre-binding model.

Supplementary Data

Supplementary Data are available at *JB* Online.

Acknowledgements

The authors thank the technicians at CNMT, JAIST, for the maintenance of research instruments. The authors also thank CNMT, JAIST, for the financial support to maintain the NMR machines used in this work. S. O. is a grant holder of JST-SENTAN.

Funding

Ministry of Education, Culture, Sports, Science and Technology (grant number 20510198); Japan Advanced Institute of Science and Technology to (S. O.).

Conflict of interest

None declared.

References

1. Nakanishi, S. (1992) Molecular diversity of glutamate receptors and implications for brain function. *Science* **258**, 597–603
2. Conn, P.J. and Pin, J.P. (1997) Pharmacology and functions of metabotropic glutamate receptors. *Annu. Rev. Pharmacol. Toxicol.* **37**, 205–237
3. Nakanishi, S., Nakajima, Y., Masu, M., Ueda, Y., Nakahara, K., Watanabe, D., Yamaguchi, S., Kawabata, S., and Okada, M. (1998) Glutamate receptor: brain function and signal transduction. *Brain Res. Brain Res. Rev.* **26**, 230–235
4. Schoepp, D.D. (2001) Unveiling the functions of presynaptic metabotropic glutamate receptors in the central nervous system. *J. Pharmacol. Exp. Ther.* **299**, 12–20
5. Enz, R. (2006) The trick of the tail: protein–protein interactions of metabotropic glutamate receptors. *BioEssay* **29**, 60–73
6. Kinoshita, A., Shigemoto, R., Ohishi, H., van der Putten, H., and Mizuno, N. (1998) Immunohistochemical localization of metabotropic glutamate receptors, mGluR 7a and mGluR 7b, in the central nervous system of the adult rat and mouse: a light and electron microscopic study. *J. Comp. Neurol.* **393**, 332–352
7. Lanthorn, T.H., Ganong, A.H., and Cotman, C.W. (1984) 2-Amino-4-phosphonobutyrate selectively blocks mossy fiber-CA3 responses in guinea pig but not rat hippocampus. *Brain Res.* **290**, 174–178
8. Bradley, S.R., Levey, A.I., Hersch, S.M., and Conn, P.J. (1996) Immunocytochemical localization of group III metabotropic glutamate receptors in the hippocampus with subtype-specific antibodies. *J. Neurosci.* **16**, 2044–2056
9. Masugi, M., Yokoi, M., Shigemoto, R., Muguruma, K., Watanabe, Y., Sansig, G., van der Putter, H., and Nakanishi, S. (1999) Metabotropic glutamate receptor subtype 7 ablation causes deficit in fear response and conditioned taste aversion. *J. Neurosci.* **19**, 955–963
10. O'Connor, V., El Far, O., Bofill-Cardona, E., Nanoff, C., Freissmuth, M., Karschin, A., Airas, J.M., Betz, H., and Boehm, S. (1999) Calmodulin dependence of presynaptic metabotropic glutamate receptor signaling. *Science* **286**, 1180–1184
11. Nakajima, Y., Yamamoto, T., Nakayama, T., and Nakanishi, S. (1999) A relationship between protein kinase C phosphorylation and calmodulin binding to the metabotropic glutamate receptor subtype 7. *J. Biol. Chem.* **274**, 27573–27577
12. Sorensen, S.D., Macek, T.A., Cai, Z., Saugstad, J.A., and Conn, P.J. (2002) Dissociation of protein kinase-mediated regulation of metabotropic glutamate receptor

7 (mGluR 7) interactions with calmodulin and regulation of mGluR 7 function. *Mol. Pharmacol.* **61**, 1303–1312
13. El Far, O., Bofill-Cardona, E., Airas, J.M., O'Connor, V., Boehm, S., Freissmuth, M., Nanoff, C., and Betz, H. (2001) Mapping of calmodulin and Gβγ binding domains within the C-terminal region of the metabotropic glutamate receptor 7A. *J. Biol. Chem.* **276**, 30662–30669
14. Ishida, H. and Vogel, H.J. (2006) Protein-peptide interaction studies demonstrate the versatility of calmodulin target protein binding. *Protein Pept. Lett.* **13**, 455–465
15. Chin, D. and Means, A.R. (2000) Calmodulin: a prototypical calcium sensor. *Trends Cell Biol.* **10**, 322–328
16. Rhoads, A.R. and Friedberg, F. (1997) Sequence motifs for calmodulin recognition. *FASEB J.* **11**, 331–340
17. Yap, K.L., Kim, J., Truong, K., Sherman, M., Yuan, T., and Ikura, M. (2000) Calmodulin target database. *J. Struct. Funct. Genomics* **1**, 8–14
18. Meador, W.E., Means, A.R., and Quiocho, F.A. (1992) Target enzyme recognition by calmodulin: 2.4 a structure of a calmodulin-peptide complex. *Science* **257**, 1251–1255
19. Scheschonka, A., Findlow, S., Schemm, R., El Far, O., Caldwell, J.H., Crump, M.P., Holden-Dye, K., O'Connor, V., Betz, H., and Werner, J.M. (2008) Structural determinants of calmodulin binding to the intracellular C-terminal domain of the metabotropic glutamate receptor 7A. *J. Biol. Chem.* **283**, 5577–5588
20. Mal, T.K., Skrynnikov, N.R., Yap, K.L., Kay, L.E., and Ikura, M. (2002) Detecting protein kinase recognition modes of calmodulin by residual dipolar couplings in solution NMR. *Biochemistry* **41**, 12899–12906
21. Airas, J.M., Betz, H., and El Far, O. (2001) PKC phosphorylation of a conserved serine residue in the C-terminus of group III metabotropic glutamate receptors inhibits calmodulin binding. *FEBS Lett.* **494**, 60–63
22. Isozumi, N. and Ohki, S. (2010) Expression and purification of metabotropic glutamate receptor 7 peptides. *Protein Expr. Purif.* **73**, 46–50
23. Putkey, J.A., Slaughter, G.R., and Means, R. (1985) Bacterial expression and characterization of proteins derived from the chicken calmodulin cDNA and a calmodulin processed gene. *J. Biol. Chem.* **260**, 4704–4712
24. Sorensen, B.R. and Shea, M.A. (1998) Interactions between domains of apo calmodulin alter calcium binding and stability. *Biochemistry* **37**, 4244–4253
25. Delaglio, F., Grzesiek, S., Vuister, G.W., Zhu, G., Pfeifer, J., and Bax, A. (1995) NMR Pipe: a multidimensional spectral processing system based on UNIX pipes. *J. Biomol. NMR* **6**, 277–293
26. Godard, T.D. and Kneller, D.G. (2006) SPARKY Version 3.113., University of California, San Francisco
27. Yang, J.J., Buck, M., Pitkeathly, M., Kotik, M., Haynie, D.T., Dobson, C.M., and Radford, S.E. (1995) Conformational properties of four peptides spanning the sequence of hen lysozyme. *J. Mol. Biol.* **252**, 483–491
28. Itzhaki, L.S., Neira, J.L., Ruiz-Sanz, J., de Part Gay, G., and Fersht, A.R. (1995) Search for nucleation sites in smaller fragments of chymotrypsin inhibitor 2. *J. Mol. Biol.* **254**, 289–304
29. Schleiff, E., Schmitz, A., McIlhinney, R.A., Manenti, S., and Vergeres, G. (1996) Myristoylation does not modulate the properties of MARCKS-related protein (MRP) in solution. *J. Biol. Chem.* **271**, 26794–26802
30. Weinreb, P.H., Zhen, W., Poon, A.W., Conway, K.A., and Lansbury, P.T. Jr (1996) NACP, a protein implicated in Alzheimer's disease and learning, is natively unfolded. *Biochemistry* **35**, 13709–13715
31. Matsubara, M., Yamauchi, E., Hayashi, N., and Taniguchi, H. (1998) MARCKS, a major protein kinase C substrate, assumes non-helical conformations both in solution and in complex with Ca^{2+}-calmodulin. *FEBS Lett.* **421**, 203–207
32. Urbauer, J.L., Short, J.H., Dow, L.K., and Wand, A.J. (1995) Structual analysis of a novel interaction by calmodulin: high-affinity binding of a peptide in the absence of calcium. *Biochemistry* **34**, 8099–8109
33. Yuan, T., Vogel, H.J., Sutherland, C., and Walsh, M.P. (1998) Characterization of the Ca^{2+}-dependent and -independent interactions between calmodulin and its binding domain of inducible nitric oxide synthase. *FEBS Lett.* **431**, 210–214
34. Wishart, D.S., Sykes, B.D., and Richards, F.M. (1992) The chemical shift index: a fast and simple method for the assignment of protein secondary structure through NMR spectroscopy. *Biochemistry* **31**, 1647–1651
35. Gellman, S.H. (1991) On the role of methionine residue in the sequence-independent recognition of nonpolar protein surfaces. *Biochemistry* **30**, 6633–6636
36. Zhang, M. and Vogel, H.J. (1994) The calmodulin-binding domain of caldesmon binds to calmodulin in an α-helical conformation. *Biochemistry* **33**, 1163–1171
37. Siivari, K., Zhang, M., Palmer, A.G. III, and Vogel, H.J. (1995) NMR studies of the methionine methyl groups in calmodulin. *FEBS Lett.* **366**, 104–108
38. Andreasen, T.J., Luetje, C.W., Heideman, W., and Storm, D.R. (1983) Purification of a novel calmodulin binding protein from bovine cerebral cortex membranes. *Biochemistry* **22**, 4615–4618
39. Baudier, J., Deloulme, J.C., Van Dorsselaer, A., and Matthes, H.W. (1991) Purification and characterization of a brain-specific protein kinase C substrate, neurogranin (p17). Identification of a consensus amino acid sequence between neurogranin and neuromodulin (GAP43) that corresponds to the protein kinase C phosphorylation site and the calmodulin-binding domain. *J. Biol. Chem.* **266**, 229–237
40. Slemmon, J.R., Morgan, J.I., Fullerton, S.M., Danho, W., Hilbush, B.S., and Wengenack, T.M. (1996) Camstatins are peptide antagonists of calmodulin based upon a conserved structural motif in PEP-19, neurogranin, and neuromodulin. *J. Biol. Chem.* **271**, 15911–15917
41. Newbell, B.J., Anderson, J.T., and Jarrett, H.W. (1997) Ca^{2+}-calmodulin binding to mouse alpha1 syntrophin: syntrophin is also a Ca^{2+}-binding protein. *Biochemistry* **36**, 1295–1305
42. Ruan, J., Xie, Q., Hutchinson, N., Cho, H., Wolfe, G.C., and Nathan, C. (1996) Inducible nitric oxide synthase requires both the canonical calmodulin-binding domain and additional sequences in order to bind calmodulin and produce nitric oxide in the absence of free Ca^{2+}. *J. Biol. Chem.* **271**, 22679–22686
43. Dasgupta, M., Honeycutt, T., and Blumenthal, D.K. (1989) The gamma-subunit of skeletal muscle phosphorylase kinase contains two noncontiguous domains that act in concert to bind calmodulin. *J. Biol. Chem.* **264**, 17156–17163
44. Yamniuk, A.P. and Vogel, H.J. (2004) Calmodulin's flexibility allows for promiscuity in its interactions with target proteins and peptides. *Mol. Biotechnol.* **27**, 33–57
45. Yuan, T., Walsh, M.P., Sutherland, C., Fabian, H., and Vogel, H.J. (1999) Calcium-dependent and -independent interaction of the calmodulin-binding domain of cyclic nucleotide phosphodiesterase with calmodulin. *Biochemistry* **38**, 1446–1455
46. Bahler, M. and Rhoads, A. (2001) Calmodulin signaling via the IQ motif. *FEBS Lett.* **513**, 107–113

47. Houdusse, A. and Cohen, C. (1995) Target sequence recognition by the calmodulin superfamily: implications from light cahin binding to the regulatory domain of scallop myosin. *Proc. Natl. Acad. Sci.* **92**, 10644–10647
48. Ishida, H., Borman, M.A., Ostrander, J., Vogel, H.J., and MacDonald, J.A. (2008) Solution structure of the calponin homology (CH) domain from the smoothelin-like 1 protein. *J. Biol. Chem.* **283**, 20569–20578
49. Vetter, S.W. and Leclerc, E. (2003) Novel aspects of calmodulin target recognition and activation. *Eur. J. Biochem.* **270**, 404–414
50. Mal, T.K., Skrynnikov, N.R., Yap, K.L., Kay, L.E., and Ikura, M. (2002) Detecting protein kinase recognition modes of calmodulin by residual dipolar couplings in solution NMR. *Biochemistry* **41**, 12899–12906
51. Schneggenburger, R. and Neher, E. (2005) Presynaptic calcium and control of vesicle fusion. *Curr. Opin. Neurobiol.* **15**, 266–274